Schweizerische Eidgenossenschaft
Confédération suisse
Confederazione Svizzera
Confederaziun svizra

Federal Department of the Environment, Transport, Energy and Communications DETEC

Swiss Federal Office of Energy SFOE
Energy Research and Cleantech

Yearly report 2023

Ice-Grid

Implementation of ice storage tanks into 5GDHC networks as seasonal storage or load shifting element

INSTITUT FÜR SOLARTECHNIK

OST Ostschweizer Fachhochschule

Date: December 11, 2023

Place: Rapperswil

Publisher:

Swiss Federal Office of Energy SFOE
Research Programme Solar Heat and Heat Storages
CH-3003 Bern
www.bfe.admin.ch
energieforschung@bfe.admin.ch

Agent:

Institut für Solartechnik SPF, Ostschweizer Fachhochschule OST
Oberseestr. 10
CH-8640 Rapperswil
www.spf.ch

Authors:

Alex Hobé, alex.hobe@ost.ch
Damian Birchler, damian.birchler@ost.ch
Florian Ruesch, florian.ruesch@ost.ch
Daniel Carbonell, dani.carbonell@ost.ch

Collaborators:

Maike Schubert
Martin Neugebauer

SFOE Head of domain: Andreas Eckmanns, andreas.eckmanns@bfe.admin.ch
SFOE Programme manager: Stephan A. Mathez, stephan.a.mathez@solarcampus.ch
SFOE Contract number: SI/502280-01

Contents

List of abbreviations and acronyms

DHW	Domestic Hot Water
EZL	Energie ZürichseeLinth
HP	Heat Pump
HX	Heat Exchanger
HTF	Heat Transfer Fluid
SH	Space Heating
WWTP	Waste-Water Treatment Plant
CS	Constant Source
SPF	Seasonal Performance Factor
DH	District Heating

1 Introduction

1.1 Low temperature thermal networks and potential of ice storages

Traditional thermal networks deliver usable supply temperatures for room heating and domestic hot water with a temperature of the heat transfer fluid of 70 °C and more. Due to the high temperatures the thermal losses of those networks are high and they are not an economic option for the less densely populated agglomeration of cities. Besides that, renewable sources for high temperature heat are limited (e.g., wood, waste incineration, waste heat or renewable fuels) and many high temperature thermal networks with renewable sources cover about 10 % to 20 % of their demand with fossil burners (Nussbaumer et al., 2017).

Anergy networks are thermal grids with working temperatures of 25 °C and lower. While in German speaking countries the terms "Anergienetz" (anergy network) or "Niedertemperaturnetz" (low temperature network) are common, in an international context such networks are often referred to as 5th Generation District Heating and Cooling or 5GDHC networks (Buffa et al., 2019). 5GDHC are a relatively new thermal network type. However, since 2010 the number of 5GDHC networks has increased. Fig. 1 shows the distribution of thermal networks in Switzerland classified by their temperature levels over time. In the future a further increase in the employment of 5GDHC networks is expected (Sres and Nussbaumer, 2014). In general, lower temperatures in thermal networks call for higher mass flow rates which in turn increase the costs for electricity in circulation pumps and the installation of piping due to the requirement of larger diameters. On the other hand, reducing the temperature reduces heat losses and eliminates the need of pipe insulation.

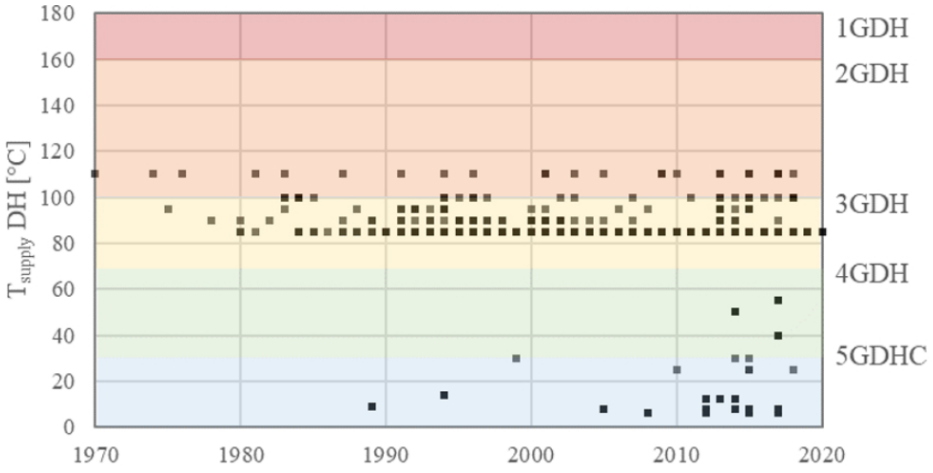

Figure 1: Distribution of Swiss thermal networks classified by estimated temperature levels (Caputo et al., 2021).

Their low operational temperatures potentially allow 5GDHC networks to use a wide range of heat sources. Research is needed on the advantanges and shortcomings of combining different heat sources with 5GDHC networks. Furthermore, how these grids will cover the winter peak loads needs to be investigated. About 40 % of the potential of heat sources for 5GDHC come from limited sources like sewage plants, ground-water, rivers, geothermal or heat rejected from cooling demands, e.g., from data centers (Sres and Nussbaumer, 2014). The use of limited heat sources in thermal networks often means a shortage in winter periods. On the other hand, excess heat is often available in summer. Therefore, seasonal thermal energy storages that can shift heat at the network level from summer to winter are necessary to cover the high thermal demand in winter, thus reducing fossil fuel needs.

Different kinds of seasonal thermal energy storages are used today, including sensible, ground and aquifer thermal energy storages. Water has a sensible storage capacity of 1.17 kWh/(m^{3}K). Assuming a temperature difference of 30 K results in an energy storage density of 35 kWh/m^3. Pit storages filled with gravel and water,

soil or rocks have a lower energy storage density (Haller and Ruesch, 2019).

Using ice storage concepts the latent heat of the fusion of water of 92.4 kWh/m^3 can be exploited. Considering that the maximum ice fraction will be limited to around 50 % to 80 %, the energy storage density is in the range of 80 kWh/m^3 to 110 kWh/m^3 considering latent and sensible heat with maximum temperature of 30 °C. Ice storages have smaller thermal losses compared to the other options listed above as they are operated for long periods at a temperature of 0 °C. Indeed gains from the surrounding ground are expected in winter.

An ice storage within a 5GDHC network can have two main functions: i) as seasonal storage to shift excess summer heat into winter and ii) as a short term storage to cover peak demands on very cold days. If the storage is used as short term storage for peak coverage, solar heat via uncovered or PVT collectors or ambient air via air heat exchangers can be used for regenerating the ice storage when available or possible. Moreover, using the short-term capacity of ice storages within thermal networks can help stabilizing the heat supply in the thermal network and to improve the flexibility that thermal networks can offer to the electricity grid.

1.2 Purpose of the project

The use of low temperature sources for thermal networks increased by a factor of 10 between 2010 and 2020, especially in districts with low energy density, where low temperature networks are preferable to higher temperature sources (Hangartner and Ködel, 2021). Prognoses from Sres and Nussbaumer (2014) expect a use of 17 TWh per year from low temperature heat sources in the year 2050 in Switzerland. This would result in a further increase of the use of low temperature sources by a factor of 9 between 2020 and 2050 (Hangartner and Ködel, 2021). From our point of view, the main potential of using ice storages in 5GDHC is its use in networks with a limited low temperature heat source such as waste heat from sewage plants, or low-grade temperature water from ground or rivers. According to Hangartner and Ködel (2021) 15 % of the energy for low temperature thermal networks (1.9 TWh/a) will be supplied from sewage plants in the year 2050, an additional 15 % will be provided from rivers. In places where no other heat source is available one can use solar thermal or PVT or an air heat exchanger for regenerating the ice storage. A third option is to use waste heat from cooling (e.g., office buildings, data centers) as a heat source to regenerate the ice storage in summer storing this heat and using it later in winter as source for the heat pumps.

Another appealing aspect of 5GDHC networks is the fact that they can be employed both for heating and cooling. Ice storages provide an interesting alternative to the borehole storages conventionally used in such applications. As the main share of cooling is provided at a temperature around 0 °C, the use of latent heat of the ice storage allows direct cooling not only for climatization but also for some industrial applications. The regeneration of boreholes, on the other hand, needs temperatures of 25 °C to 30 °C which strongly limits the direct/free cooling potential (Ruesch and Haller, 2017). In an unpublished feasibility study, we have carried out a simplified calculation for a 5GDHC on an hourly base showing that an ice storage of 700 m^3 with a 400 kW air heat exchanger as the only heat source can replace 4600 m of ground probes. The costs for the ice storage in combination with the air heat exchanger are estimated to be 270 000 CHF compared to about 350 000 CHF for the ground probes, representing a costs reduction of 20 %.

In the SFOE project BigIce (Carbonell et al., 2021), the energetic potential of solar-ice systems for multi-family buildings was shown. Seasonal performance factors of about 4 can be reached all over Switzerland with well dimensioned systems. The concept of a solar-ice system will be scaled and adapted to low temperature thermal networks in the project Ice-Grid. Hence, in the current project the combination of an ice storage with solar thermal collectors as the only renewable heat source for a low temperature thermal network will be explored, too. Furthermore, variations such as using centralized/decentralized concepts for the solar field and heat pump with a centralized ice storage concept will be investigated. To avoid repetition of work and following Open Science principles, we will make our simulation framework publicly available, facilitating the further development and uptake of these concepts in the research community.

1.3 Project objectives

The goal of this project is to quantify the potential of ice storage tanks used within 5GDHC networks. Ice storage tanks are expected to be a benefit in 5GDHC with limited heat sources. Different combinations of heat

sources will be analyzed using detailed dynamic system simulations with *TRNSYS*. Possible heat sources are waste heat of sewage plants, air heat exchangers and solar thermal or PVT collectors. Both centralized and decentralized heat sources will be tested. The most important factors influencing the performance of thermal networks with ice storage tanks will be identified. The results of the simulation study will lead to decision criteria and design rules for the consideration of ice storage tanks in early planning stages.

The objectives of the project are:

- Describe typical network configurations with large potential for the implementation of ice storage tanks.
- Analyse the cost-energetic potential of ice storages in 5GDHC networks. The focus will be on identifying the main influencing factors on the performance of thermal networks with an integrated ice storage.
- Give simple rules for the implementation and the dimensioning of ice storages in thermal networks considering both long-term as well as short-term storage concepts.
- Quantify the cost-economic potential of the implementation of ice storages in real low temperature thermal networks by analysing case studies together with simulations.

2 Case Study: EZL Anergy Network in Jona

2.1 Modeling the EZL district heating network

2.1.1 Topology implementation

Fig. 2 shows the topology of the District Heating (DH) network operated by Energie ZürichseeLinth (EZL) in Jona, Switzerland.

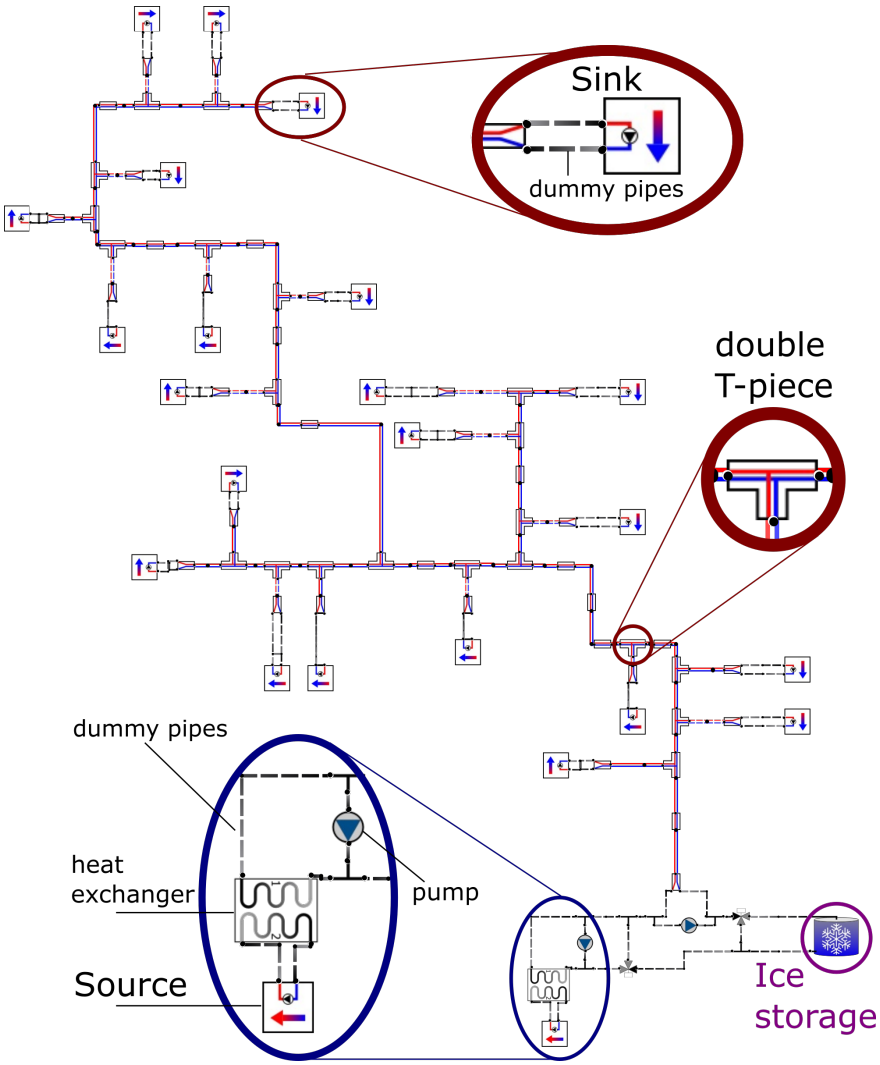

Figure 2: Topology of the modeled EZL district-heating network in Jona. Indicated are: **Sinks:** These group consumers into a single heat sink with a single heat pump and sink specific demand profiles. **Double T-pieces:** These divert both hot and cold pipes to the sinks. **Ice storage:** This provides sensible and latent heat to shift heating demands. **Source:** An ARA source provides the network's heat through a heat exchanger. The pump recirculates the carrier fluid (ethanol) to ensure the water in the ARA side never drops below its freezing point. **Dummy pipes:** Pipes with dashed lines are "dummy pipes": they don't exhibit any thermal losses and don't have any heat capacity. Fig. 3 provides further detail on the bottom part of the diagram.

The model network consists of 19 sinks connected in parallel via double pipes (three of the 22 sinks shown

in Fig. 2 currently do not have demands). The double pipes model heating of their surrounding soil and losses or gains to and from the environment beyond the modeled soil layer. The return flow from the network is routed through the ice storage before it is returned to the source in the lower left of Fig. 2. When there is less demand in the network than the source is supplying, the ice store can be actively regenerated by imposing additional flow in the regeneration pump by-passing the network supply and return (cf. Fig. 3). There is also a valve to by-pass the ice storage in case it is fully frozen.

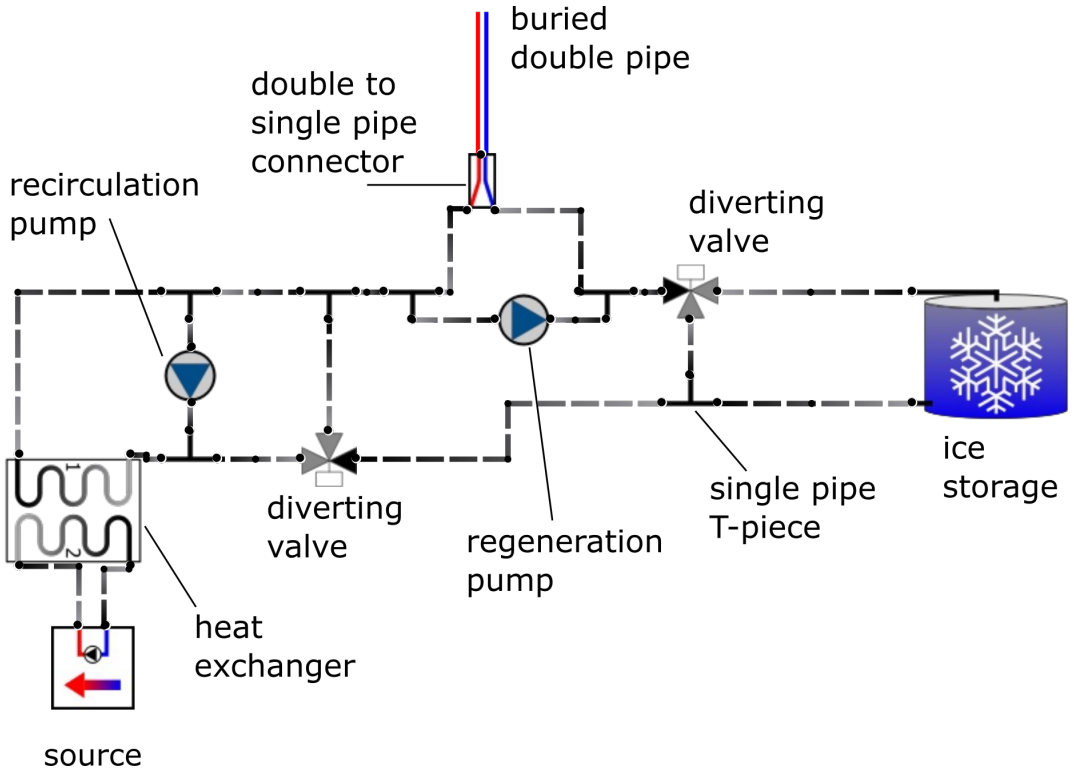

Figure 3: Central components at the source location of the modeled EZL district-heating network in Jona. Besides the source and ice storage, these components are mainly needed for temperature control. See Section 2.1.4 for further explanation.

If the network temperature is too low, there is a danger of freezing the treated waste water in the Heat Exchanger (HX) with the Waste-Water Treatment Plant (WWTP). In that case, the recirculation pump is activated (i.e. set to a constant positive mass flow) and the diverting valve just before the HX is controlled to ensure the HX inlet temperature at the network side does not decrease below 2 °C. Freezing danger on the water bearing side of the HX (the side of the WWTP) is therefore avoided with some margin of security. The valve before the HX can also be used to additionally control the return temperature of the source side of the HX, e.g. if we want to control for a fixed temperature difference over the source side, as would typically be the case for a Constant Source (CS).

2.1.2 Sinks description

The simulation is simplified by grouping individual costumers along a network leg into so-called "sinks" (Fig. 2). Each of the sinks is defined by: 1) a Heat Pump (HP) with a nominal power equal to the design capacity of the network leg represented by the sink, 2) demand profiles for Domestic Hot Water (DHW) and Space Heating (SH), 3) a storage tank for hot water and for space heating, which is used as a simple one-node building model/storage to capture the thermal capacity of the buildings connected to the network leg.

The internal storages are scaled according to the maximum yearly demand of the sink. The DHW is scaled to provide half an hour of the maximum demand, whereas the heat capacity of the buildings is set to two

hours of maximum SH demand.

The design capacities of the network legs were provided by EZL. From these, the demand profiles were generated using a demand calculation tool developed at SPF (Ruesch and Haller, 2022). To generate a profile the tool takes into account: 1) weather data, 2) HP capacity, 3) total yearly demand, 4) the fraction of the total demand needed for DHW and SH and the heating limit. Fig. 4 shows example profiles for one of the sinks.

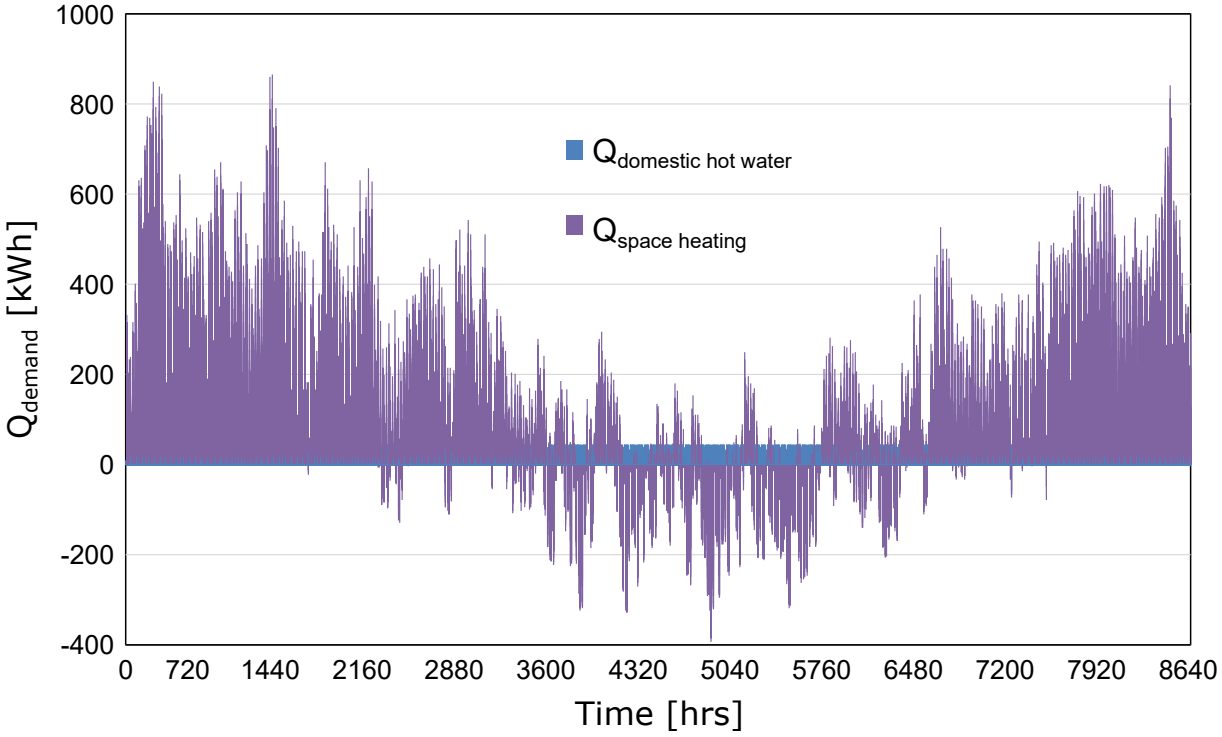

Figure 4: Example of hourly demand profiles for DHW and SH for a full year. Currently, cooling demands are ignored.

The storages represent a part of the boundary of our simulation model: the demands are directly withdrawn from the storages, i.e. the heating distribution systems are not simulated. The HPs are controlled based on the storage temperatures by an on/off two-point controller with hysteresis. When a storage temperature drops below its minimum allowed temperature, the heat pump is turned on. The heat pump continues running until the storage temperature has reached a certain maximum temperature. At which stage, the heat pump turns off and remains off until the storage temperature falls below the minimum allowed temperature again. If both storages need charging, the DHW storage is prioritized over the SH/building storage.

The grid provides heat at a low temperature to the HPs. The HPs lift that heat to the desired temperatures of the storages (SH: 37 °C, DHW: 60 °C). Due to their differing demand profiles, the sinks require different amounts of heat at different times. This, together with the storages's thermal inertia, helps to smooth out the total heat demand in the system.

2.1.3 Ice storage

The role of the ice storage is - as with any kind of heat storage - to store heat in times of excess heat supply in order to release it again when the supply cannot cover the demand. An ice storage will release heat at around zero degrees Celsius when the water contained in the storage freezes. For example, when the Heat Transfer Fluid (HTF) of the network is around −5 °C in winter, it is circulated through the internal heat exchanger of the ice storage. The HTF operated at this temperature will freeze some of the water in the storage while

being heated up itself due to the enthalpy of fusion released when the water in the storage freezes. Usually, the HTF would leave the ice storage heated to temperatures slightly below zero, e.g. −0.5 °C.

The storage is re-charged when the ice in the storage is melted again. In case of active regeneration, the ice storage is partially charged and molten frequently. The complete melting process (until fully charged) usually starts in spring. Of course, the storage can also be charged and discharged in the absence of any freezing or melting: liquid water in the storage can simply be heated and cooled. The main point of an ice storage is that the freezing process allows to store ∼80 times more heat, as the fusion enthalpy of water at zero degrees Celsius (333 kJ kg^{-1}) is ∼80 times larger than the heat capacity of water achieved for a temperature difference of 1 Kelvin (4.19 kJ kg^{-1} K^{-1}). Therefore, freezing 1 kg of water releases the same amount of energy as cooling the same amount of water from 80 °C to 0 °C. In the thermal networks we analyze, the maximum temperature an ice storage can reach is about 20 °C. Thus, about four times more heat can be extracted by using latent heat compared to using sensible heat.

As can be seen in Fig. 3, the ice storage is placed at the return of the network, just before the HTF is sent through the source HX to be heated up and circulated through the network once more. At the return of the network, the highest mass flow of the return fluid is achieved. Therefore, it is at that location in the network where the ice storage provides the most power. If it is technically possible to place the ice storage there, it is recommended to do so. The effect of storage locations other than the one currently investigated and, in particular, the effect of multiple distributed storages would be an interesting topic for further investigation. To prevent "overfreezing" of the ice storage, a valve is installed to circumvent the storage if needed. If the ice storage is completely frozen, however, the system runs into the following problem. The demand is no longer shifted by the ice storage, so either the source can meet all of it, or the network temperature will drop and freezing would occur at the WWTP HX.

2.1.4 Source description and control

Two different kinds of sources were investigated: 1) a source for which the return temperature must not fall below 2 °C and 2) a source for which the return temperature must not be lower than the supply temperature by more than a given temperature difference. The first case corresponds to a WWTP source, where the 2 °C lower bound is used to avoid freezing in the source side of the heat exchanger. The second case represents a constant source of low temperature waste heat as for example from industrial processes or cooling of IT-infrastructure.

The outflow temperature of the WWTP source is modeled as a sine function over the year:

$$T_{src,out} = 17\,^{\circ}\mathrm{C} + 4\,^{\circ}\mathrm{C}\sin\left(\frac{t-751}{8761}\cdot 2\pi + \frac{3\pi}{2}\right) \tag{1}$$

where t is time in hours. The source temperature thus oscillates between 13 °C and 21 °C to account for temperature differences over the seasons, with the minimum temperature occurring on February 1st. For the generic sonstant source, a constant supply temperature of 15 °C was assumed. Constant mass flows throughout the year of 430 210 kg h^{-1} and 1 500 000 kg h^{-1} were assumed for the WWTP source and the constant waste source, respectively.

In both cases, a heat exchanger is used to integrate the sourcs into the DH network.

Care must be taken not to freeze the treated waste water in the heat exchanger with the WWTP. At times of high demand (typically during winter) a drop below 0 °C is allowed in the constant power source case. While the ice storage is not fully frozen, it will - to some degree - buffer the drop below 0 °C in the temperature of the HTF. Regardless, even with the ice storage active, temperatures slightly below zero degrees Celsius can often be observed in times of high demand.[1] Therefore, in order to prevent freezing and potential damage to the heat exchanger, the inlet temperature on the network side of the heat exchanger needs to be controlled.

2.2 Parameter Studies

Using the *pytrnsys* simulation framework developed at SPF, different parameterizations of the system shown in Fig 2 were simulated. For both sources, the demand, storage size (including no storage) and the mode

[1] When the ice storage is fully frozen and has to be bypassed, the temperature in the network drops quite rapidly to temperatures significantly (e.g. −7 °C) below zero. Such a scenario is not sustainable for long, as the heat pumps cannot support too low an inlet temperature at the evaporator.

of regeneration (i.e. active vs. passive) were simultaneously varied. To vary the demand, all profiles were multiplied by the same scaling factor.

We additionally carried out a specific search in the parameter space to obtain the optimum storage size for a given demand. Here, the source capacity is first exhausted, as zero costs is the optimum when the existing infrastructure can meet the demand. Beyond the source capacity, the optimum storage size is the one that just reaches the maximum allowed ice ratio of ∼80 % for a given demand.

2.2.1 Parametric studies results

To find out how the parametric studies could be carried out, different approaches were followed. The complexity for these simulations come from 1) having no back up solution that could compensate for insufficient ice storage capacity and ii) that the scaling factors of the ice storage were unknown. Actually, one of our goals is to find out how one can scale the ice storage for different types of anergy networks and therefore our scaling factor decision will be one of the outcomes of the project.

Originally, we were simulating using many absolute ice storage volumes. This lead to situations in which many cases needed no ice storage but were simulated and many other cases either failed or had very low ice fractions. An example using absolute ice storage volumes for the WWTP case with active regeneration is shown in Fig. 5 using the total heat demand Q_d on the x-axis.

Fig. 5a shows the ratio of the used latent heat capacity of the ice storage in MWh and the total heat demand in GWh. The latent heat is not used until approximately a Q_d between 17 GWh to 18 GWh. A similar plot but using the maximum amount of water frozen in tonns, which can be read as m^3 too, is shown in Fig. 5c. Since the latent heat of fusion is approximately 92 kWh/tonn, the two plots differ by this factor on the y-axis. From those, one reads that, e.g. for 30 GWh of demand we need an ice storage volume around 100 m^3 or ∼8 MWh/GWh, which corresponds to 240 MWh of latent heat capacity.

Fig. 5d shows the mass ice fraction, i.e. the maximum amount of water (in mass) that is converted into ice. For an ice-on-coil storage, one could assume that, for safety reasons, the maximum ice fraction should not exceed 80 %. Above this value, the ice expansion might lead to damages of the storage vessel. From these results we can observe that the ice fraction rarely goes above 50 % and thus, in most of the cases, the ice storage volume is not used efficiently. The latent-to-sensible capacity ratio used in the ice storage is shown in Fig. 5f. For most of these simulations, the sensible term is even higher than the latent one and as maximum we get a ratio below 3 for an ice storage volume of 2951 m^3 and a Q_d around 27 GWh. These low latent-to-sensible heat ratios are related to the over-sizing of the ice storages.

In Fig. 5e we present the average SPF_{hp} of all heat pumps on the network. We can observe a drop on the overall heat pump efficiency as the demand increases since longer freezing times of the ice storage are necessary and therefore the network is operated at temperatures of around 0 °C for longer durations.

In summary, the main problem of these simulations is that the ice storage is mostly over-sized and the question is: *how can we scale the simulations in such a way, that the ice fraction reaches reasonable values, while varying the demand, without having to run thousands of simulations?* One proposition for a generalisation of the results was to use the latent capacity of the ice storage in MWh with respect to the GWh of total demand, as shown in Fig. 5a. However, we have seen that the sensible part is not insignificant and therefore it might be used for a better scaling approach. With this idea in mind we plotted the (used) latent and sensible capacity of the ice storage, $Q_{lat}+Q_{sen}$ with respect to Q_d in Fig. 5b. From these plots one could read that we would need storage capacities below 15 MWh/GWh to achieve proper ice storage sizing, for the WWTP cases.

Fig. 5 shows that scaling factors using the latent and sensible heat capacity of the ice storage could provide good insights on sizing needs. However, the use of the total heat demand Q_d is very case dependent, since each network will have a different demand in which the ice storage is necessary. As an idea to circumvent this particularity, the x-axis was scaled using the additional heat demand Q_{add}, defined as the total heat demand minus the threshold demand where the latent part of the ice storage is not necessary. Basically, we would like to plot the simulations over an axis where $Q_{add} \leq 0$ GWh represents the cases where the network does not need an ice storage. Using the results in Fig. 5 to calculate Q_{add}, we chose a threshold demand of 18 GWh.

Fig. 6 shows the adjusted plots using the chosen Q_{add} as the scaling unit. Besides the change in the x-axis, all values that use GWh as a scaling unit, i.e MWh/GWh and $tonn_{ice}$/GWh are affected by this modification.

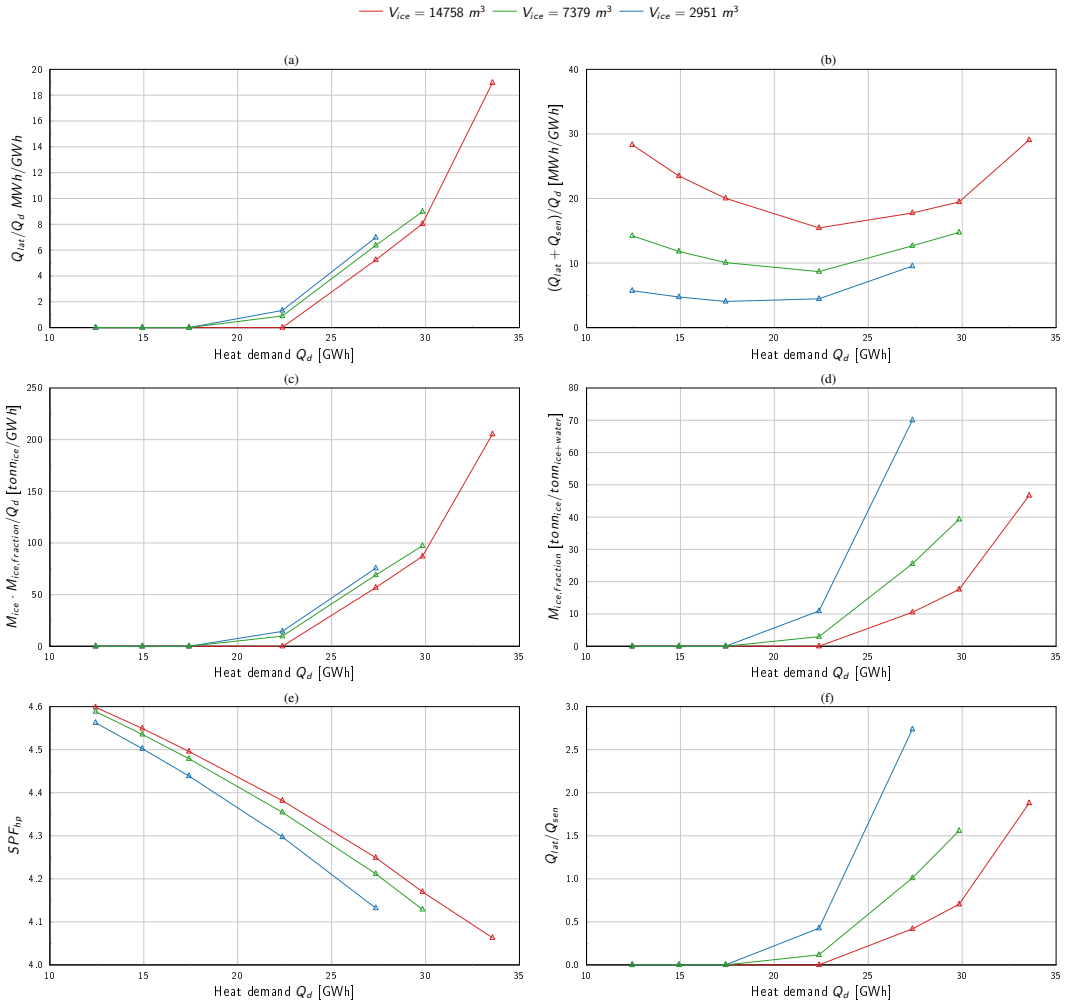

Figure 5: Results for WWTP with active regeneration as a function of the total heat demand, while varying the absolute ice storage volumes.

Fig. 6b is especially interesting. It shows the latent and sensible capacity of the ice storage scaled by Q_{add}. These lines are not increasing as a function of Q_{add}, like Q_{lat} in Fig. 6a does. Therefore, it seem to be a good scaling factor for running the parametric studies with the aim to get ice storage volumes that are close to the 80 % ice fraction target.

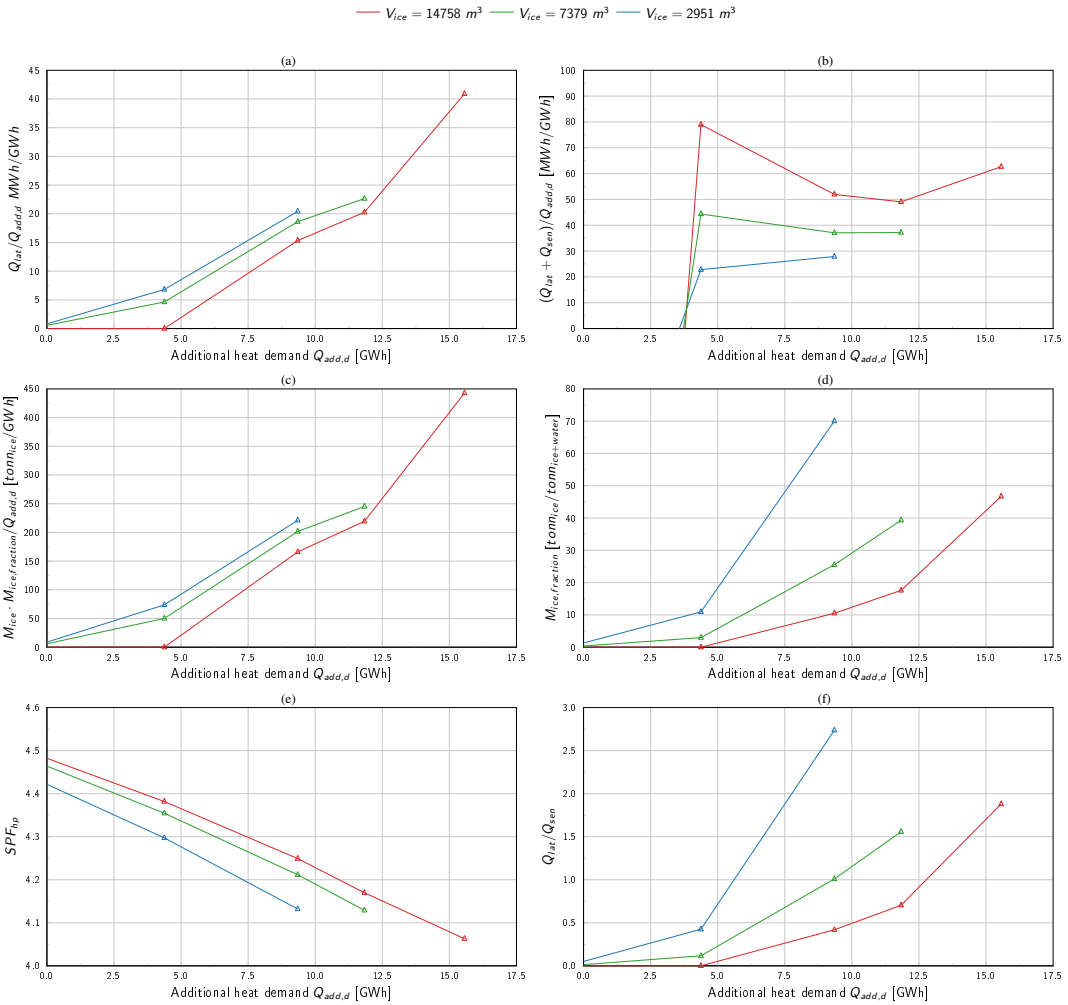

Figure 6: Results for WWTP with active regeneration as a function of the additional heat demand, while varying the absolute ice storage volumes.

We therefore did another parameter study using $(Q_{lat}+Q_{sen})/Q_{add}$ in MWh/GWh as the scaling factor with values ranging from 20 MWh/GWh to 50 MWh/GWh. As the actual results were still unknown beforehand, these values were calculated assuming a maximum ice fraction of 70 % to prevent too many simulations from failing. Fig. 7 shows the results of this latest parameter study for the WWTP case using active regeneration. With the proposed scaling factor, we obtain at least one simulation for each demand, which is close to the desired maximum ice-fraction (Fig. 7d).

Fig. 7b shows the calculated scaling-factor values from the results obtained using the assumed scaling factors shown in the legend. Unfortunately, the values used to scale the total demand and the heat demand values obtained in the simulations are not identical, leading to possible confusions in interpreting the results. One might expect that cases where the ice fraction is equal to 70 % in Fig. 7d would lead to a condition in which the scaling factor used to size the ice storage shown in the legend would be equal to the value obtained in the y-axis of Fig. 7b. This small deviation will be solved by re-simulating all results next year with improved

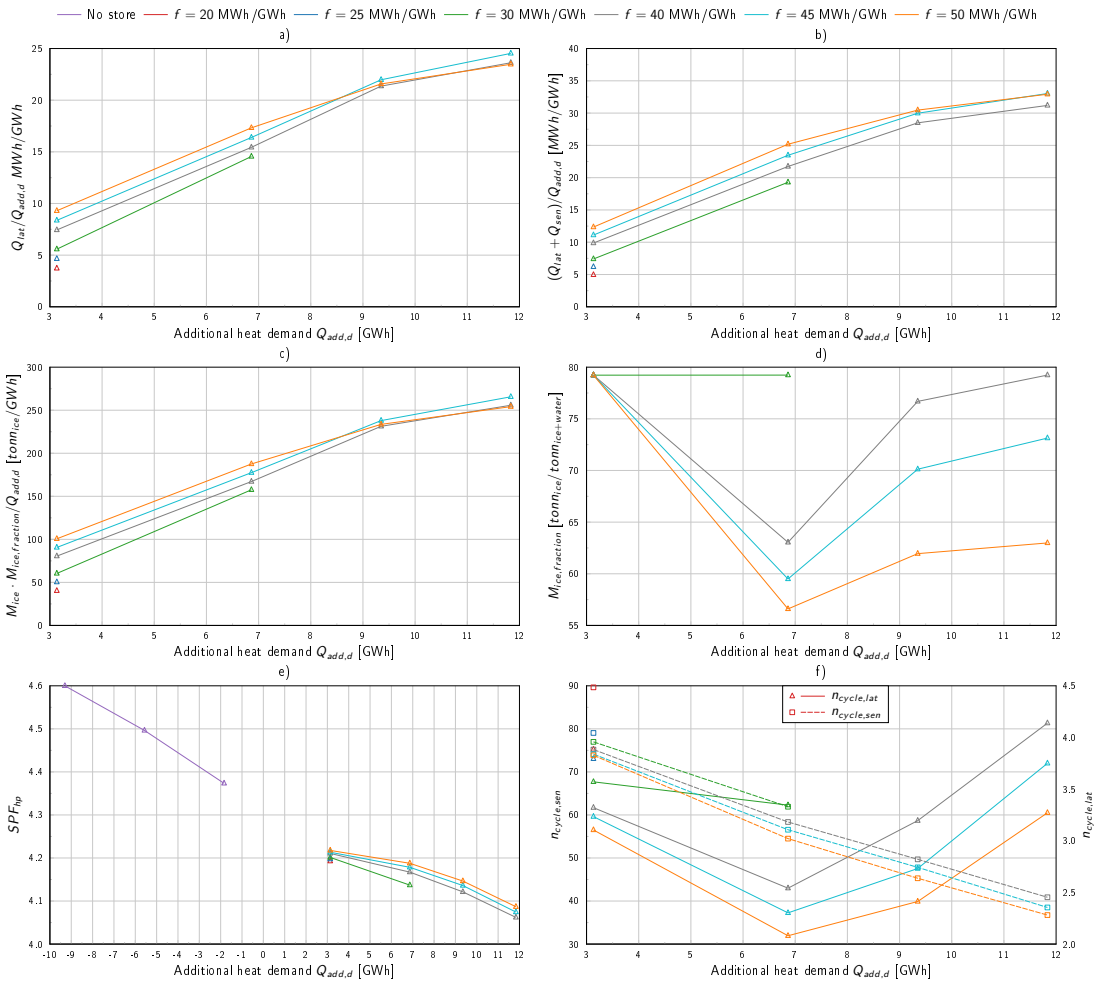

Figure 7: Results for the Waste-Water Treatment Plant (WWTP) case with active regeneration.

scaling-demand factors, based on these promising results. One result that needs some further explanation from Fig. 7d is that all scaling-factors used at Q_{add} of $\sim$3 GWh achieve the maximum ice fraction around 80 % allowed in the simulation model. These are cases with a relatively small absolute ice storage volume compared to the whole thermal network capacity and thus, these ice storages freeze quickly during few days of a peak demand in January. The difference between the storages sizes is compensated with the thermal grid inertia, operating with lower network temperature for smaller ice storage on peak period times. On these cases, despite of operating at lower temperatures, the heat pumps can still run without a failure[2]. Instead, in future simulations, we will limit the minimum temperature the thermal grid.

The SPF_{hp} is shown in Fig. 7e where the cases simulated without an ice storage have been included. We have left a gap between the plots with and without an ice storage. The chosen ice-storage capacities for this range where always too large, which lead to the ice storage only working as a sensible storage. For the time being we have eliminated those cases. In future simulations, we will include appropriate ice storage sizes to cover this gap.

Compared to previous figures, Fig. 7f shows a new plot where the number of cycles of the storage are shown. The number of cycles are calculated as the energy delivered by the storage divided by its specific capacity. The latent heat capacity is calculated assuming a 100 % mass ice fraction, while the sensible capacity is calculated using the maximum temperature of the storage (20 °C). Fig. 7f shows the sensible cycles (left y-axis) in dashed lines. The solid lines show the number of cycles using latent energy (right y-axis). Interestingly, the number of cycles using sensible energy range from 40 to 80 approximately, while the latent heat capacity is used between 2 to 4 times.

[2] Typical heat pumps accept evaporator brine temperature in the range of −6 °C to −8 °C.

Fig. 8 shows same results presented above, but for the case in which the ice storage is not actively regenerated. In this case the size of the storage needs to be significantly higher with scaling factors between 120 MWh/GWh to 150 MWh/GWh. For this case we achieve ice fractions above 70 % in all demands except the one at ∼10 GWh, where it can be observed in all plots a kind-of discontinuity on the results.

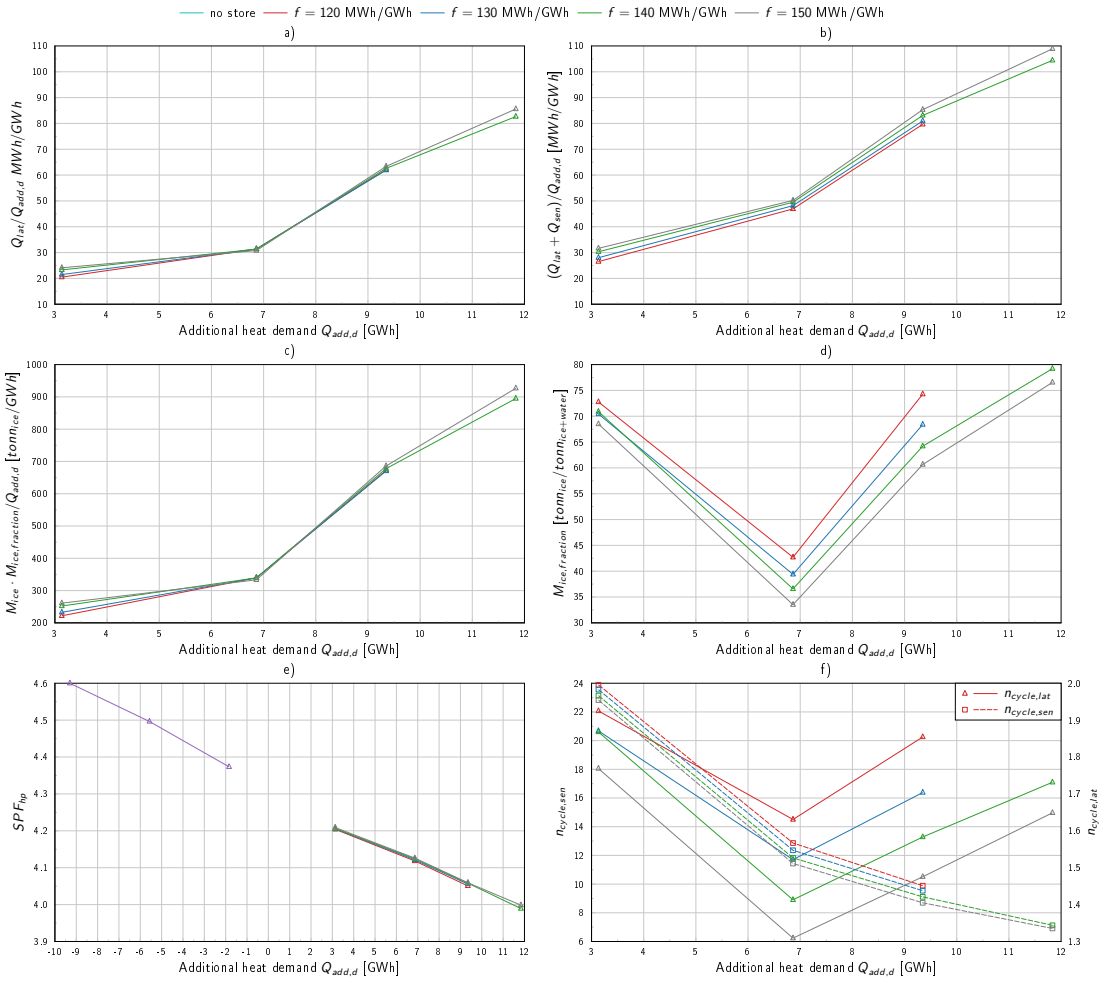

Figure 8: Results for the Waste-Water Treatment Plant (WWTP) case without active regeneration.

In the following, results for the Constant Source (CS) case are presented. The main difference between the cases is the heat source, which is a WWTP in one and a generic constant source in the other case.

Fig. 7 displays the active regeneration results for the Constant Source (CS) case. For these cases high mass fractions above 75 % can be achieved with only two scaled ice storage volumes of 25 kWh/GWh and 30 kWh/GWh. Thus, ice storage sizes are smaller compared to the Waste-Water Treatment Plant (WWTP) case. The main reason is the higher number of cycles achieved using the CS source case, which range from 50 to 100, compared to the WWTP heat source, which range from 40 to 75 for the sensible part.

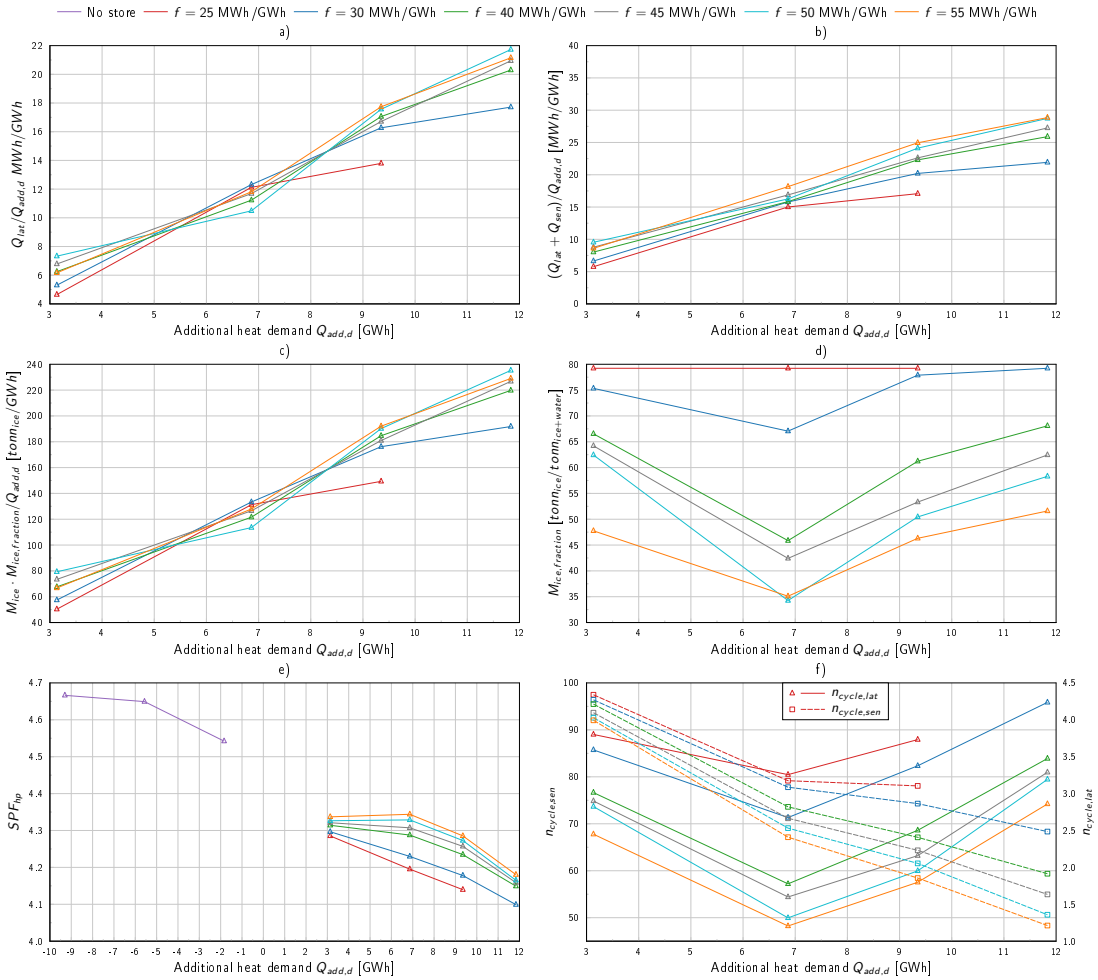

Figure 9: Results for the Constant Source (CS) case with active regeneration

.

Fig. 8 displays the passive regeneration results for the Constant Source (CS) case. With the used ice storage scaling factors from 150 MWh/GWh to 180 MWh/GWh, the last added demand of 11.8 GWh could not be achieved. Thus, without active regeneration, the Constant Source (CS) needs higher ice storages compared to the Waste-Water Treatment Plant (WWTP) source. This is also in line with the lower number of cycles achieved in the CS case, which range from 8 to 24 for the sensible part.

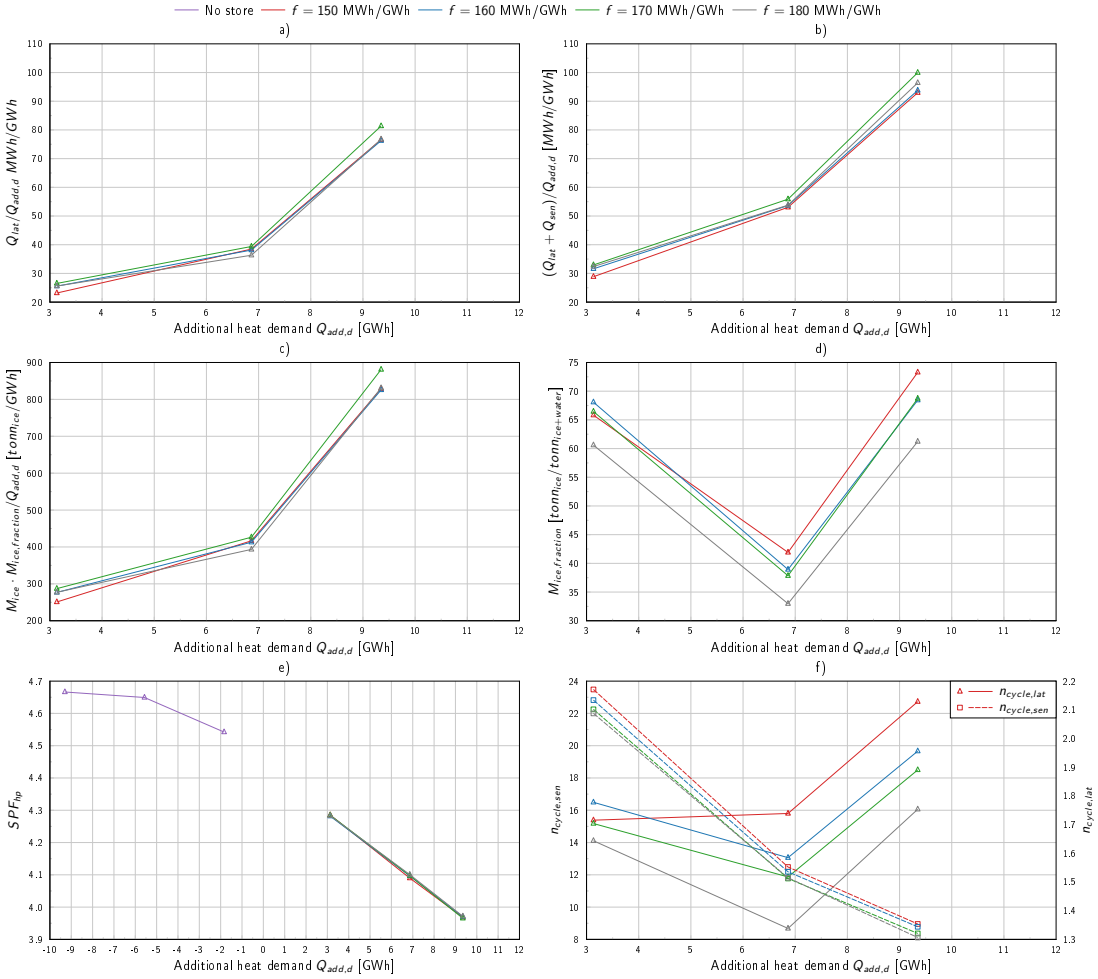

Figure 10: Results for the Constant Source (CS) case without active regeneration

.

2.2.2 SPF comparisons between active and passive regeneration

Fig. 11 compares the Seasonal Performance Factor (SPF) for both active and passive regeneration in the WWTP case. Here, the SPF decreases linearly with increasing demand, even before the cross-over point ($Q_{add,d}$=0). For low added demands ($Q_{add,d}$=3), both active and passive regeneration have very similar SPF values. As $Q_{add,d}$ increases further, the SPF values of the active regeneration cases diverge non-linearly from the linear trend of both the network without storage ($Q_{add,d}$<0) and the passive regeneration cases. Interestingly, the SPF values of the passive regeneration cases is robust against over-sizing the storage. In other words, there is no added benefit of having an over-sized storage from an SPF standpoint when using passive regeneration.

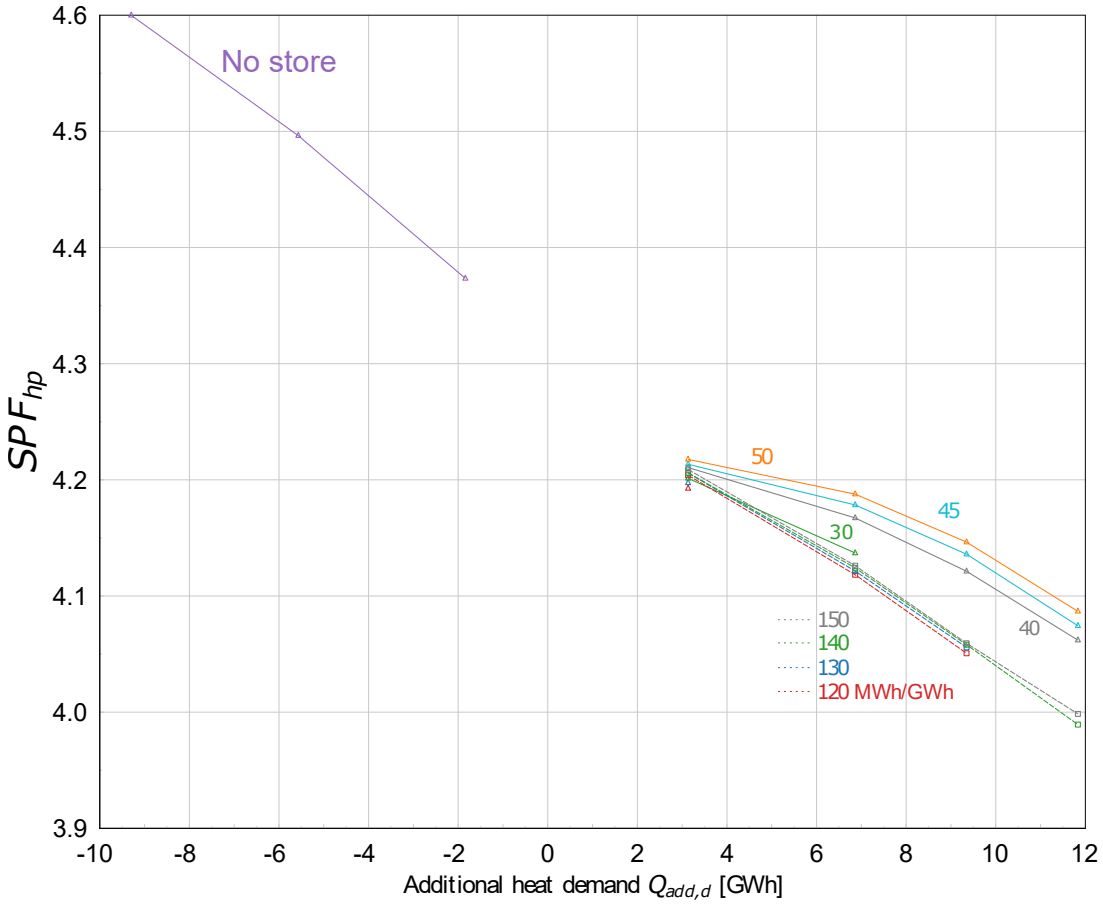

Figure 11: Comparison of active (solid lines) and passive (dashed lines) generation results for the Waste-Water Treatment Plant (WWTP) case, focusing on Seasonal Performance Factors (SPFs) as a function of additional heat demand ($Q_{add,d}$), which is defined as the demand above the maximum demand, that the source can meet by itself. Colors show the relative size of the ice storage for each simulation.

For the active regeneration cases, Fig. 11 shows a stronger dependence of the SPF on the storage size. As the storage size increases, given the same demand, the SPF increases with it. The improvement in the SPF from the active respect to the passive case is mainly due to the increased number of equivalent cycles the storage is used in these simulations. This can be observed in Fig. 7f and Fig. 8f, where it can be read that the number of sensible cycles for the active regeneration range from 30 to 110, while in the passive case, the cycles reduce in the range of 5 to 35.

The increased SPF values for the active regeneration cases are obtained using much smaller storage volumes. This promising result would allow network operators to meet the same demand with a smaller storage, when active regeneration is used, increasing the levelized cost of the storage. However there is a need of additional pumping energy, which has not been analysed in detail yet.

Fig. 12 displays the SPF for both active and passive regeneration in the Constant Source (CS) case. Qualitatively, the results are very similar to those of the Waste-Water Treatment Plant (WWTP) case (Fig. 11).

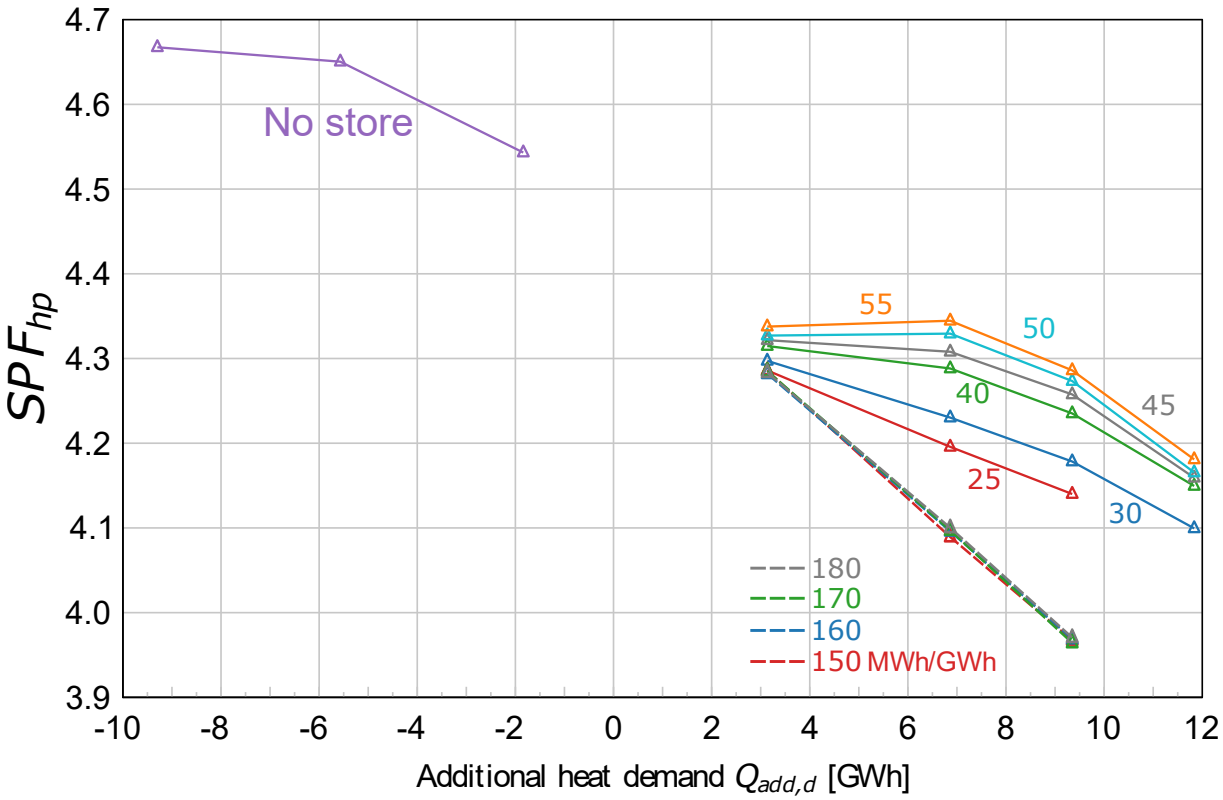

Figure 12: Seasonal Performance Factors (SPFs) as a function of additional heat demand ($Q_{add,d}$) for the active (solid lines) and passive (dashed lines) generation results for the Constant Source (CS) case. Q_{add} is defined as the demand above the maximum demand, that the source can meet by itself. Colours show the relative size of the ice storage for each simulation.

The SPF drops with increased demand before the cross-over point ($Q_{add,d}=0$), and the active regeneration cases diverge non-linearly from the passive regeneration cases. The are three bigger differences to the Waste-Water Treatment Plant (WWTP) case: 1) the SPF values are generally higher, 2) the passive regeneration cases have a faster decrease in SPF as demand increases, and 3) the SPF values decrease non-linearly with increasing demands for cases without storage ($Q_{add,d}<0$). Though the active regeneration cases seem to diverge more strongly for the CS case, these cases actually also have a stronger decrease in SPF values with increasing demands compared to the Waste-Water Treatment Plant (WWTP) case (cf. Figs. 11 and 12).

We advice against drawing deeper conclusions from a direct comparison between the Constant Source (CS) case and the Waste-Water Treatment Plant (WWTP) case at this time. As the CS case has a limited temperature drop over the heat exchanger, the mass-flow rates on the source side of the heat exchanger are increased to get to the same source power. This fundamentally alters the energies transmitted over the heat exchanger, and with them, how the simulations ultimately behave. Nevertheless, the qualitative assessments are very similar for these cases.

3 Sizing rules for cost-optimum cases

In the cases examined, dimensioning an ice-storage system in a cost optimal way means finding the smallest possible ice-storage volume for a given demand, which does not lead to freezing or malfunction in the attached components. From the simulations presented in Fig. 7 for the Waste-Water Treatment Plant (WWTP) case with active regeneration, we have selected those that achieve an ice fraction above 75 % (Fig. 13). When more than one solution exist, the lowest ice storage volume is chosen.

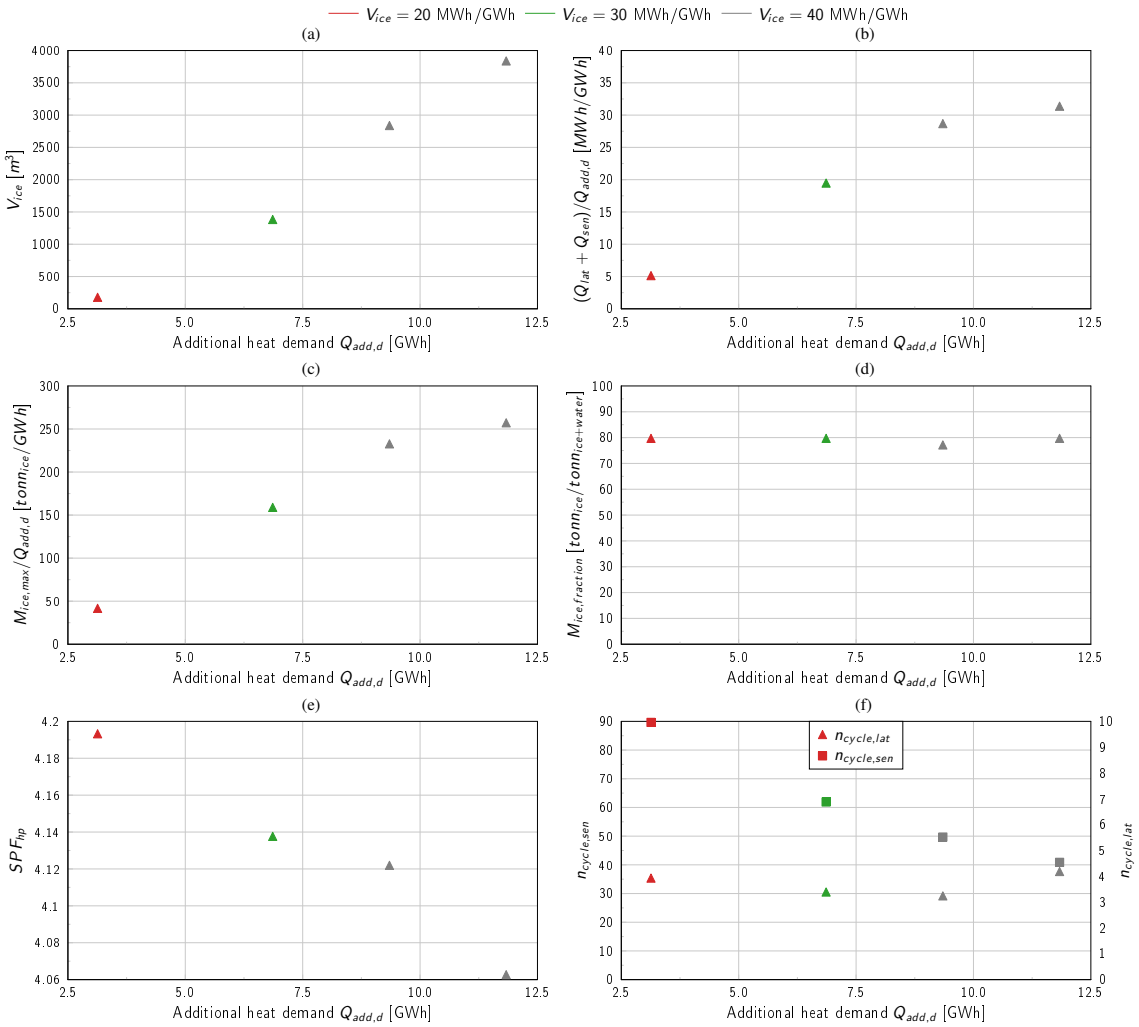

Figure 13: Cost-optimal ice-storage sizes for the Waste-Water Treatment Plant (WWTP) case with active regeneration.

In Fig. 13f we can observe that all cases achieve ice fractions in the range of 80 %. Fig. 13b indicates which sizing factors should be used to achieve cost-optimal solutions for the present case with scaled storage sizes ranging from 5 MWh/GWh to 30 MWh/GWh. For $Q_{add,d}$ <9 GWh, the scaling of the ice storage is quite linear; After that, it tends to become of second order. The absolute ice-storage volumes are presented in Fig. 13a with values ranging from 200 m^3 to 3800 m^3. Fig. 13c displays the maximum mass of frozen water in tonns, which could be read as m^3 too. Thus, ice-storage volumes of 50 m^3/GWh to 250 m^3/GWh are necessary for this case. As an order of magnitude, solar-ice systems need between 400 m^3/GWh to 1000 m^3/GWh, where the GWh refers to the total heat demands (i.e. space heating and DHW combined). Fig. 13f shows the sensible and latent number of cycles achieved for all cases with values ranging from 3 to 4 with respect to the latent

capacity and between 40 and 90 for the sensible capacity. The large number of cycles show that the ice storages are still far from being seasonal in this application. Seasonal storages tend to have cycles close to 2. This is, indeed, a large benefit of the ice storage for this application, since the larger the cycles, the better the levelised cost of storage.

The evolution of the mass ice fraction over the year for the four selected cases are presented in Fig. 14a. From this plot, it can be seen that, the higher the demand, the wider the profile of the mass ice fraction. The heat demand has one large peak in January and one in February and, for all cases, the mass of ice peaks on these periods. After the January peak demand period, there is enough heat source from the WWTP to regenerate the ice storage. For all cases except for the largest demand of 11.8 GWh, all the ice storages are completely melted before they are partially frozen again at around 9500 h. At around 1000 h, the February peak demand appears and all ice storages are partially frozen again. For the highest demand of 11.8 GWh, the ice storage is in frozen mode for larger periods, being just melted before the second peak demand in February at around 1000 h.

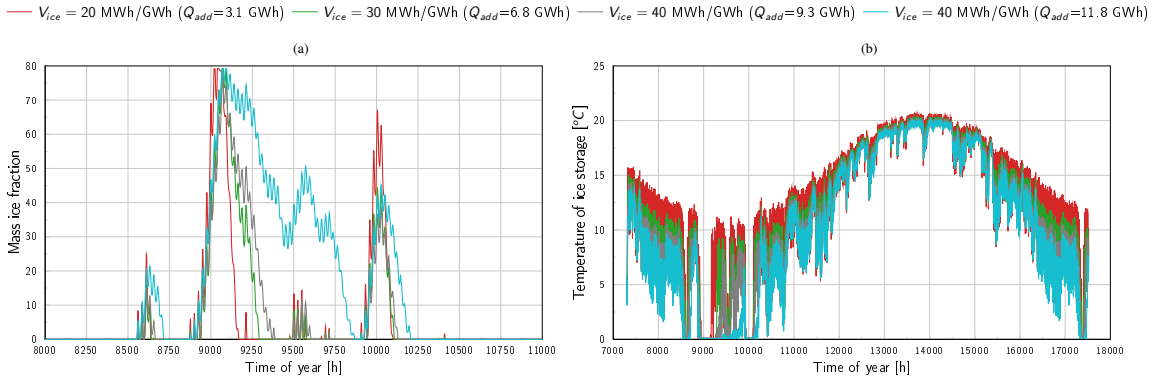

Figure 14: (a) Ice mass fraction evolution over the second winter of the simulations for selected ice storage volumes for the four Q_{add} demands and (b) ice storage temperature for the whole simulation period.

The temperature of the ice storage over the year is displayed in Fig. 14b. First of all we can observe that for all cases a maximum temperature of 20 °C is reach in summer due to the warm temperature of the WWTP source. Moreover, there are a lot of fluctuations of temperature all year round, except on the small period where ice is formed. Even in winter, in between the two peak demands at around 9000 h and 1000 h, the number of cycles of the ice storage, with the exception of the largest demand of 11.8 GWh, is large. This explains the large number of cycles on the sensible part. The large number of sensible cycles are related to the daily temperature variations induced by fluctuation's in the demand profiles. In future simulations, different daily profiles of demand and source will be analysed to assess the effects on sizing factors.

From the results presented above we can conclude that a simple function can be derived to asses the cost optimal (minimal) size of the storage for this thermal network. However, this function will not be developed until more cases with different boundary conditions are simulated to assess the generality of the sizing rules. Moreover, we have not reach yet the limit of how far we can extend the demand of the thermal grid using an ice storage for the Waste-Water Treatment Plant (WWTP) case with active regeneration, which we will do next year.

Simulations from Fig. 8 show that, ice storage sizes in the range of 30 MWh/GWh to 110 MWh/GWh are needed in combination with passive regeneration, compared to sizes in the ranges of 5 MWh/GWh to 35 MWh/GWh for active regeneration. Thus, active regeneration can reduction ice storage volumes by a factor of 3 to 6. Benefits of the active regeneration will depends strongly on the heat source profile, both daily and seasonally.

4 National / International cooperation

The project involves cooperation with several industrial partners. The main collaboration during 2023 was with EZL, which operates the Jona heating network, with whom we exchanged a lot of useful information and had fruitful discussions. Interim results from the project were repeatedly presented and discussed at meetings as part of the SWEET project "DeCarbCH" (within Work package 3). It is planned to use the Jona heating network from the IceGrids project as a benchmark case for the comparison of different simulation and modelling tools within the DeCarbCH consortium. The project and interim results were also presented at the SPF Symposium Solar Energy and Heat Pumps (November 2, 2023, Rapperswil).

Cooperation is also taking place with SPF's own BigStoreDH project. In BigStoreDH, the extensions of *pytrnsys* developed here were used to simplify the simulation of classic heating networks. On the other hand, the methods for creating typical load profiles developed in BigStoreDH were used in this project. The extension of the *pytrnsys* GUI developed in the project for DH networks was announced both nationally (to the DeCarbCH partners) and internationally (at IEA-SHC Task 68). It is intended to be shared with all *pytrnsys* users.

5 Evaluation of 2023 and Outlook final report

The simulation models and tools developed and validated in 2022 were used in 2023 both for the EZL case study and for the parameter studies carried out. The idea is to generate a large number of reliable results to be able to find out sizing rules for dimensioning ice storages for low temperature DH networks.

Several issues with the modeling framework were identified and corrected through the concrete implementation of the hydraulic diagram of the Jona heating network in the pytrnsys GUI with more than 20 decentralized consumers distributed over several network legs. For example, it was found that with a large network, detailed modeling of all connections between the network and consumers using only pipes, led to small time steps and therefore impractically long simulation times. For this reason, simple connectors or "dummy pipes" were introduced to enable these connections without slowing down the simulation.

The current and specifically planned expansion of the Jona heating network, which can be supplied by the capacity of the ARA even without an ice storage, was mapped and simulated. As the EZL is planning a further expansion of the network, the demand was further increased and it was shown that an expansion to 20 GWh is possible with the integration of an ice-storage system. However, a lowering of the grid temperature below the freezing point of water must be accepted, which is technically possible as the network already uses a heat transfer fluid with antifreeze. As soon as the network temperature drops below zero degrees Celsius, an ice-storage tank can be integrated directly into the grid without an additional heat pump. By adding water from the network supply, the temperature of the WWTP heat exchanger could be kept above freezing despite the direct integration of the ice-storage tank.

The results for the Jona case study were received with interest by EZL. In this specific case, however, contractual obligations regarding grid temperature make concrete implementation difficult, and it is therefore unlikely that an ice storage will be implemented with the further expansion of the Jona grid. However, EZL is planning two further WWTP grids, where the integration of an ice storage will be included already in the planning phase for the advanced-expansion stages.

The results obtained for the EZL case study were generalized through further parameter variations and standardization. For example, different loading and regeneration strategies were analyzed. An analysis with constant source power provides a further generalization of the results. A constant source power can be, for example, waste heat from industrial processes or the cooling of IT infrastructure (i.e. server farms). The investigated parameter variations and generalizations allow a rough dimensioning of the ice-storage system for a planned network expansion beyond the existing capacity of a low-temperature source. The results also show the efficiency losses (reduction in the COP of the heat pumps) that must be expected when expanding the supplied heat demand, even without an ice storage. Our results show that these efficiency losses can be reduced slightly by maximizing the latent and sensible cycles of an ice storage using active regeneration. Until the end of the project, these dimensioning rules will be refined further on the basis of additional variations in

demand and source specifics (including solar and ambient air). Furthermore, we will specify the framework conditions within which the rough design rules and estimates are valid.

References

Buffa, S., Cozzini, M., D'antoni, M., Baratieri, M., and Fedrizzi, R. (2019). 5th generation district heating and cooling systems: A review of existing cases in Europe. *Renewable and Sustainable Energy Reviews*, 104:504–522.

Caputo, P., Ferla, G., Belliardi, M., and Cereghetti, N. (2021). District thermal systems: State of the art and promising evolutive scenarios. A focus on Italy and Switzerland. 65:102579.

Carbonell, D., Schubert, M., and Neugebauer, M. (2021). *Big-Ice - Assessment of solar-ice systems for multi-family buildings*. Institut für Solartechnik SPF for Swiss Federal Office of Energy (SFOE), Research Programme Solar Heat and Heat Storage, CH-3003 Bern.

Haller, M. and Ruesch, F. (2019). Fokusstudie "Saisonale Wärmespeicher - Stand der Technik und Ausblick".

Hangartner, D. and Ködel, Ködel, K. (2021). Liste "Thermische Netze". Technical Report Energie Schweiz.

Nussbaumer, T., Thalmann, S., Jenni, A., and Ködel, J. (2017). Planungshandbuch Fernwärme. Technical report.

Ruesch, F. and Haller, M. (2017). Potential and limitations of using low-temperature district heating and cooling networks for direct cooling of buildings. 122:1099 – 1104.

Ruesch, F. and Haller, M. (2022). Jahresbericht 2022, bigstoredh. Technical report.

Sres, A. and Nussbaumer, B. (2014). Weissbuch Fernwärme Schweiz - VFS Strategie.